The Plant Cell, Vol. 22: 3177–3187, September 2010, www.plantcell.org

Tissue-Adapted Invasion Strategies of the Rice Blast Fungus *Magnaporthe oryzae* [W]

Sylvain Marcel,[a,1] Ruairidh Sawers,[a,2] Edward Oakeley,[b,3] Herbert Angliker,[b] and Uta Paszkowski[a,4]

[a] Department of Plant Molecular Biology, University of Lausanne, CH-1015 Lausanne, Switzerland
[b] Friedrich Miescher Institute for Biomedical Research, CH-4058 Basel, Switzerland

***Magnaporthe oryzae* causes rice blast, the most serious foliar fungal disease of cultivated rice (*Oryza sativa*). During hemibiotrophic leaf infection, the pathogen simultaneously combines biotrophic and necrotrophic growth. Here, we provide cytological and molecular evidence that, in contrast to leaf tissue infection, the fungus adopts a uniquely biotrophic infection strategy in roots for a prolonged period and spreads without causing a loss of host cell viability. Consistent with a biotrophic lifestyle, intracellularly growing hyphae of *M. oryzae* are surrounded by a plant-derived membrane. Global, temporal gene expression analysis used to monitor rice responses to progressive root infection revealed a rapid but transient induction of basal defense-related gene transcripts, indicating perception of the pathogen by the rice root. Early defense gene induction was followed by suppression at the onset of intracellular fungal growth, consistent with the biotrophic nature of root invasion. By contrast, during foliar infection, the vast majority of these transcripts continued to accumulate or increased in abundance. Furthermore, induction of necrotrophy-associated genes during early tissue penetration, previously observed in infected leaves, was not seen in roots. Collectively, our results not only report a global characterization of transcriptional root responses to a biotrophic fungal pathogen but also provide initial evidence for tissue-adapted fungal infection strategies.**

INTRODUCTION

Rice blast disease, caused by *Magnaporthe oryzae*, can lead to the loss of up to 30% of annual rice (*Oryza sativa*) yield (Talbot, 2003). Due to the agronomic importance of rice, understanding the molecular mechanisms underlying infection by this pathogen is of utmost importance. In general, the outcome of plant–pathogen interactions depends on a molecular interplay between the two organisms, with the pathogen attempting to control the plant cell for the establishment of a compatible interaction (Schulze-Lefert and Panstruga, 2003). To gain access to nutrients, plant pathogens have evolved different lifestyles; biotrophs derive their needs from living host cells, whereas necrotrophs destroy host tissue for their own nourishment (Lewis, 1973; Glazebrook, 2005). *M. oryzae* belongs to an intermediate class, the hemibiotrophic pathogens, combining biotrophic and necrotrophic features. Typically, hemibiotrophs initially grow biotrophically and then switch to necrotrophic growth, killing the infected tissues (Perfect and Green, 2001; Munch et al., 2008). *M. oryzae*, however, invades foliar tissue by maintaining both lifestyles simultaneously (Kankanala et al., 2007). Leaf infection by *M. oryzae* initiates from a conidium that adheres to the leaf surface. Germination of the conidium produces the germ tube that further develops into a melanized appressorium from where a penetration peg enters the epidermal cell by mechanical piercing of the cell surface (Wilson and Talbot, 2009). Inside the cell lumen, bulbous and intensively dividing invasive hyphae (IH) become surrounded by a plant-derived membrane that separates the IH and host cytoplasm, a characteristic of biotrophy (Kankanala et al., 2007). Fungal progression to the next cell occurs in the vicinity of pit fields without causing visible damage to the cell wall, the fungus likely crossing the cell wall at plasmodesmata (Kankanala et al., 2007). Fungal invasion of neighboring cells coincides with the loss of cell viability of the previously infected cell and the onset of necrotrophic growth leading to the appearance of lesions, typically, by 74 to 96 h after inoculation under laboratory conditions (Berruyer et al., 2006; Wilson and Talbot, 2009). Although major rice resistance (*R*) and corresponding *M. oryzae* avirulence genes have been identified (Valent et al., 1991; Farman et al., 2002), mechanisms underlying susceptibility remain unknown. Transcriptome analysis on leaf material enriched for IH identified the first biotrophy-associated secreted proteins from *M. oryzae* and a number of rice encoded genes corresponding to potential compatibility factors (Mosquera et al., 2009).

The phylogenetically close relationship between *M. oryzae* and soil-borne root pathogens of the Magnaporthaceae (Cannon, 1994), such as *Magnaporthe poae* and *Magnaporthe rhizophila* (pathogens of Kentucky bluegrass and millet, respectively) as well as *Gaeumannomyces graminis* (a pathogen of wheat)

[1] Current address: Institute for Plant Genomics and Biotechnology, Texas A&M University, College Station, TX 77843-2123.
[2] Current address: Laboratorio Nacional de Genómica para la Biodiversidad, Irapuato, 36500 Irapuato, Mexico.
[3] Current address: Novartis Institutes for BioMedical Research, CH-4056 Basel, Switzerland.
[4] Address correspondence to uta.paszkowski@unil.ch.
The author responsible for distribution of materials integral to the findings presented in this article in accordance with the policy described in the Instructions for Authors (www.plantcell.org) is: Uta Paszkowski (uta.paszkowski@unil.ch).
[W] Online version contains Web-only data.
www.plantcell.org/cgi/doi/10.1105/tpc.110.078048

suggested that, similar to its relatives, *M. oryzae* also retained the ability to infect roots. Although the distribution of *M. oryzae* in the soil is currently not well characterized, competence of *M. oryzae* to colonize roots efficiently has been recognized (Dufresne and Osbourn, 2001). *Magnaporthe* has been considered a hyphopodiate genus (Landschoot and Jackson, 1989; i.e., members form hyphopodia, simple hyphal swellings that mediate root penetration). For example *G. graminis*, the economically important take-all pathogen of wheat, is a well-studied relative of *M. oryzae* that invades roots via hyphopodia that form on hyphae colonizing the root surface (Asher and Shipton, 1981). As could have been expected, *M. oryzae* also initiates root infection from simple hyphopodia without formation of a specialized infection structure (Sesma and Osbourn, 2004; Tucker et al., 2010). However, *M. oryzae* employs an additional developmental program for appressoria differentiation during leaf infection, a feature that *G. graminis*, for example, lacks. The ability to use either hyphopodia or appressoria thus permits *M. oryzae* to adapt its penetration mechanisms to the properties of the target organ, which in consequence raises questions as to the degree of similarity between leaf and root infection strategies. Over recent years it has become clear that the fungal genetic tool box of *M. oryzae* includes a combination of common and organ-specific components to accomplish initial penetration of either the cuticle-covered leaf epidermis or the rhizodermis (Dufresne and Osbourn, 2001; Sesma and Osbourn, 2004; Tucker et al., 2010). However, the intraradical development of the fungus has not been fully characterized. Standard microscopy investigations have lead to the suggestion that the fungus passes the rhizodermis and the root cortex by inter- and intracellular growth, likely following a hemibiotrophic strategy comparable to that in leaves (Sesma and Osbourn, 2004; Heupel et al., 2010; Tucker et al., 2010). Furthermore, the fungus has been observed finally to enter into the central cylinder of the root from where it systemically spreads throughout the plant (Sesma and Osbourn, 2004), and, following prolonged cocultivation of 2 to 4 weeks, blast symptoms have been observed on both roots and on aerial organs of root-inoculated plants, thereby revealing that although symptom development occurs considerably slower than on leaves, the fungus has the ability to cause disease on roots and systemically (Sesma and Osbourn, 2004). Despite its potential relevance for rice blast epidemiology, root susceptibility to *M. oryzae* receives little attention and thus remains poorly explored. In this study, we provide a detailed characterization of the intraradical stages of root invasion by *M. oryzae* and show that, contrary to the previous understanding, intraradical fungal proliferation from rhizodermal to vascular tissue proceeds in a strictly biotrophic fashion.

RESULTS

Morphology and Dynamics of Root Infection by *M. oryzae*

To characterize *M. oryzae* infection of rice roots, we inoculated roots of in vitro cultivated rice plants with conidia of green fluorescent protein (GFP)-expressing *M. oryzae* and documented infection over a period of 10 d by fluorescence and confocal microscopy (Figures 1A to 1F). Within 1 d after inoculation (DAI), conidia germinated, producing fungal hyphae that rapidly made physical contact with the root. By 2 DAI, numerous runner hyphae were present along the longitudinal axis of the root surface (Figure 1A) and the first fungal penetration of the rhizodermis was observed (Figures 1B and 1C). Fungal hyphae entered the tissue mainly through rhizodermal cells, but rare penetration of root hairs was also observed (Figure 1C). Consistent with previous reports, the melanized appressoria that are typically associated with leaf infection were not observed on roots (Sesma and Osbourn, 2004; Tucker et al., 2010). Instead, penetration pegs were formed from swollen hyphal structures reminiscent of hyphopodia (Figure 1B). Upon penetration, primary hyphae rapidly differentiated into thick IH and intracellularly colonized the root rhizodermis with limited hyphal branching (Figure 1D). Fungal progression was characterized by successive invasions of rhizodermal cells with no apparent loss of cell

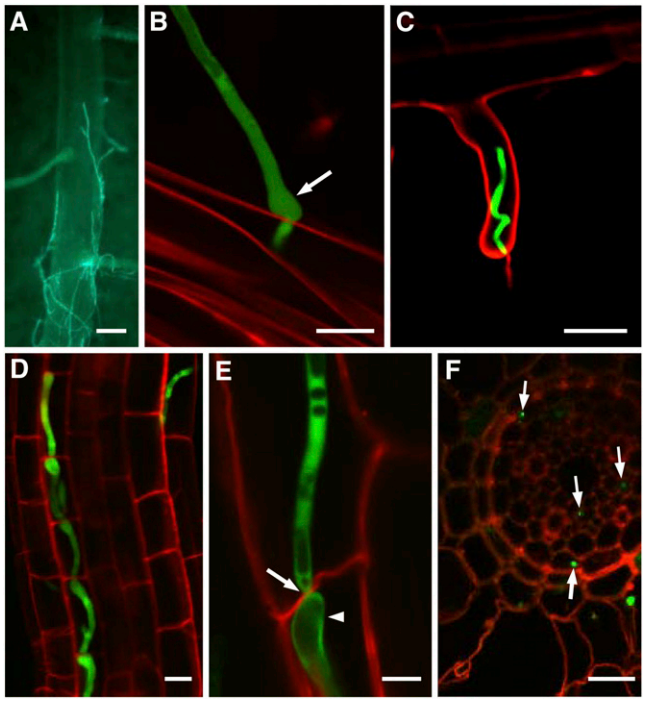

Figure 1. Morphology and Dynamics of Rice Root Colonization by GFP-Transformed *M. oryzae*.

Fluorescence stereomicroscopy **(A)** and confocal laser scanning microscopy (**[B]** to **[F]**) analysis to monitor fungal infection of rice roots. Root cell walls were stained with propidium iodide in **(B)** to **(F)**.

(A) Proliferation of runner hyphae on the root surface at 2 DAI. Bar = 50 μm.

(B) Hyphopodia formation (arrow) on the surface of the rhizodermis followed by intracellular penetration of the rhizodermal cell observed at 2 DAI. Bar = 10 μm.

(C) Fungal penetration of the rhizodermis through a root hair. Bar = 20 μm.

(D) Intracellular propagation of *M. oryzae* invasive hypha in rhizodermis at 4 DAI. Bar = 10 μm.

(E) Bulbous hypha constricts for cell wall crossing to the neighboring cell (arrow). Note swelling prior crossing (arrowhead). Bar = 5 μm.

(F) Invasion of vascular tissue observed at 6 DAI. Bar = 15 μm.

viability, as was concluded from an absence of autofluorescence (Figure 1D) and coloration of root cells upon trypan blue staining (Hermanns et al., 2003; Berrocal-Lobo and Molina, 2004; Kimbrough et al., 2004). IH became more bulbous prior to crossing the cell wall and constricted dramatically, resulting in a thin invasive peg at the point of passage (Figure 1E). In this fashion, at 6 DAI, fungal hyphae had spread to inner cell layers of the root, including the cortex, the endodermis, and the vascular tissue (Figure 1F). The different root types of the rice root system, namely, crown, large lateral, and fine lateral roots (Gutjahr et al., 2009; Rebouillat et al., 2009), were equally well colonized. Infection in independent experiments proceeded with hyphopodia formation at 2 DAI, cortex infection by 4 DAI, and entrance into the vasculature by 6 DAI. Development of disease symptoms was not observed at any point up to 10 d of in vitro cocultivation. However, on stems and leaves of >15% of root-inoculated plants, typical blast symptoms developed at 4 weeks after inoculation when rice plants were grown and inoculated in sand culture (Sesma and Osbourn, 2004). In summary, *M. oryzae* exhibited strictly intracellular invasion of all rice root cell layers and rapidly colonized the root, including the vascular tissue, without causing necrosis within the assessed period of up to 10 DAI.

M. oryzae Practices a Biotrophic Lifestyle during Rice Root Infection

In leaves, fungal growth is linked to the loss of cell viability behind the infection front (Kankanala et al., 2007). The absence of apparent cell death in infected roots prompted us to verify the viability of root cells hosting fungal structures. Infected roots were treated with the lipophilic endocytic dye FM4-64 to allow monitoring of endocytosis and endosome formation (Bolte et al., 2004). After 20 min of incubation, internalization of FM4-64 was observed in endomembrane structures that formed in a similar fashion in noninfected (Figures 2A and 2B, arrowheads) and in *M. oryzae*–infected cells (Figure 2A, arrows), indicating that intracellular fungal colonization did not affect cellular membrane dynamics and, thus, cell viability. Importantly, in contrast to leaf infection, invaded root cells remained alive once the fungus had progressed to adjacent cells, as reflected by continuous endocytotic activity (Figure 2A, arrows). It was therefore predicted that the fungus remains enveloped in a plant-derived extrainvasive hyphal membrane throughout intracellular growth. Transmission electron microscopy was performed on 8 DAI infected tissue to visualize the plant-fungal interface. The presence of an electron-dense plant-derived membrane was observed around intracellular fungal structures, acting to isolate IH from the cellular content of the host cells (Figures 2C to 2E). Crossing of the cell wall was associated with extreme hyphal constriction of the IH but without indication of damage (Figure 2E). Thus, *M. oryzae* maintains an intimate biotrophic relationship with the hosting root cell over at least 8 DAI without apparent loss of host cell viability.

The SYM Signaling Pathway Is Not Required for Intracellular Accommodation of *M. oryzae*

Biotrophic root invasion by *M. oryzae* is morphologically reminiscent of the root endosymbiosis with arbuscular mycorrhizal

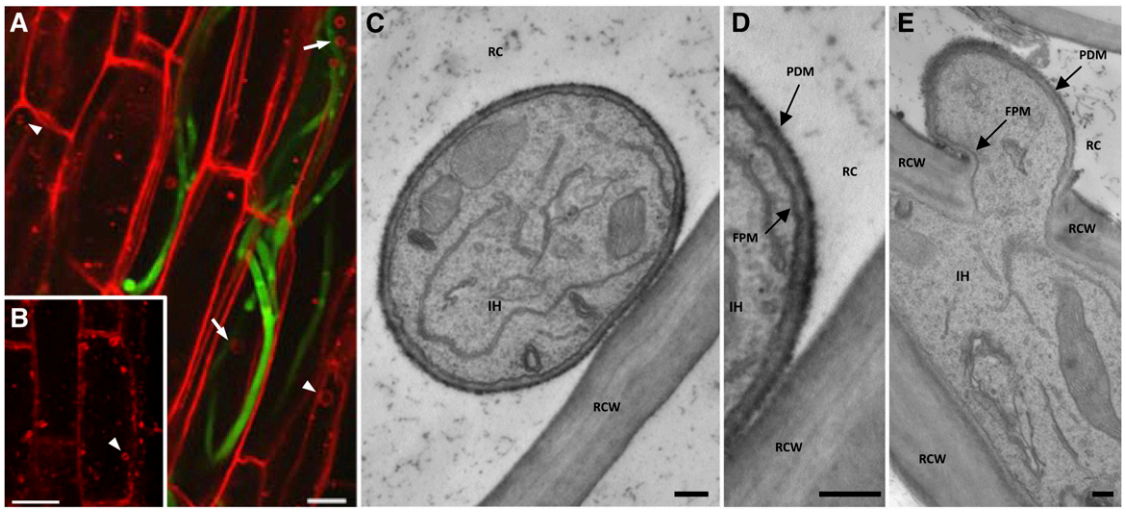

Figure 2. Microscopic Examination of Membrane Dynamics in Rice Cells Invaded by GFP-Transformed *M. oryzae*.

(A) and **(B)** Confocal laser scanning micrograph using maximum projection of a z-stack of infected **(A)** and a single projection of noninfected **(B)** root tissue at 4 DAI treated with the endocytic tracer FM4-64. Note the internalization of FM4-64 into endomembrane structures in invaded (arrows) and noninvaded (arrowheads) rhizodermal cells. Bars = 10 μm.

(C) to **(E)** Transmission electron micrographs of cross sections of infected root cells prepared at 8 DAI showing enveloping of intracellular invasive fungal hyphae by a plant-derived membrane **(C)**. The fungal-plant interface is composed of the fungal plasma membrane, the fungal cell wall, and the plant-derived membrane.

(D) Magnified transmission electron micrograph of the plant-fungal interface presented in **(C)**.

(E) Transmission electron micrograph illustrating the constriction of the IH during cell-to-cell crossing.

FPM, fungal plasma membrane; IH, invasive hypha; PDM, plant-derived membrane; RC, rice cell; RCW, rice cell wall. Bars = 200 nm.

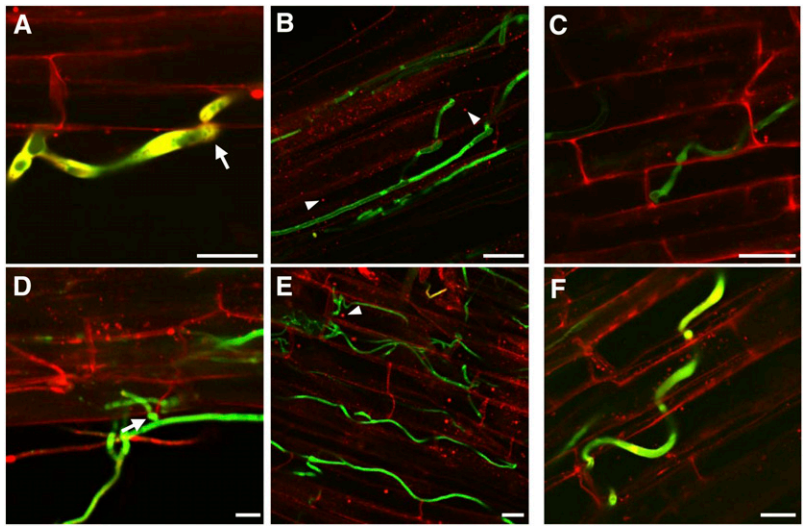

Figure 3. Confocal Laser Scanning Microscopy of Root Infection of *castor-1* and *ccamk-2* Mutants by GFP-Expressing *M. oryzae.*

Root colonization of *castor-1* (**[A]** and **[B]**), *ccamk-2* (**[D]** and **[E]**), and corresponding wild type (**[C]**, cv Dongjin; **[F]**, cv Nipponbare, respectively).
(A) and **(D)** Hyphopodia formation (arrows) on the rhizodermis of *castor-1* **(A)** and *ccamk-2* **(D)**. Cell walls were stained with propidium iodide. Bars = 10 μm.
(B), **(C)**, **(E)**, and **(F)**, Mutant (**[B]** and **[E]**) and corresponding wild type (**[C]** and **[F]**) roots stained with the endocytotic tracer FM4-64. Endocytotic vesicles (arrowheads) in *castor-1* **(B)** and *ccamk-2* **(E)** are indicative of viable invaded mutant cells. Bars = 20 μm. All images represent maximum projections of a z-stack.

(AM) fungi (Paszkowski, 2006) that requires an intact signaling pathway, termed SYM for common symbiosis signaling (Parniske, 2008), consisting of at least four genes in rice (Gutjahr et al., 2008, and citations therein). This pathway had been hypothesized to be required generally for intracellular accommodation of microbes (Parniske, 2000). We examined two representative rice *sym* mutants, *castor-1* and *ccamk-2* (Gutjahr et al., 2008), that affect the signaling cascade upstream (*castor-1*) and downstream (*ccamk-2*) of calcium spiking, a central molecular signature to signal transduction. Hyphopodia formation and intracellular growth of *M. oryzae* hyphae were unchanged in the roots of the two mutants compared with wild-type plants (Figures 3A, 3C, 3D, and 3F). Viability of the invaded cells was confirmed by FM4-64 staining (Figures 3B and 3E). Therefore, in contrast to biotrophic root colonization by AM fungi, root biotrophy of *M. oryzae* does not require an intact SYM signaling pathway.

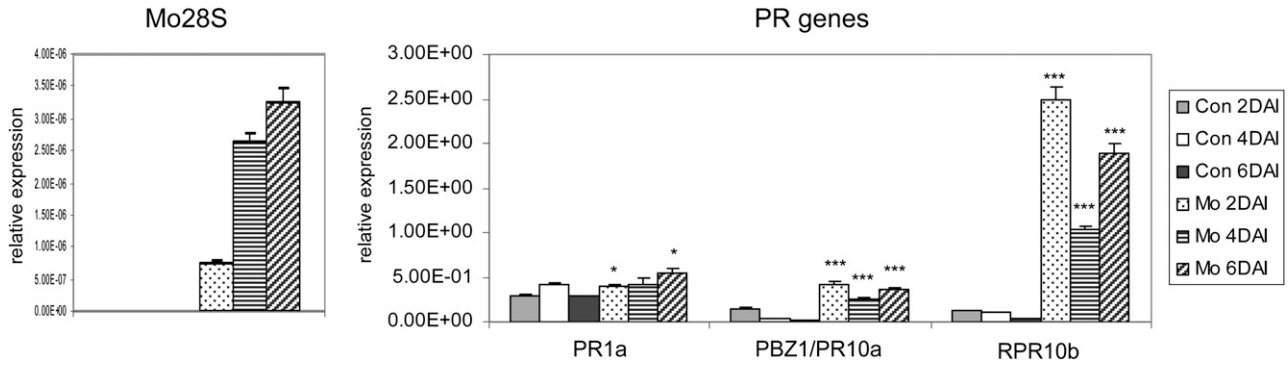

Figure 4. Real-Time RT-PCR–Based Temporal Expression Analysis of Rice and *M. oryzae* Genes during Root Invasion.

Left, constitutively expressed *M. oryzae* ribosomal 28S cDNA monitors the increasing amount of intra- and extraradical fungal proliferation (Qi and Yang, 2002); right, root invasion by *M. oryzae* leads to increased transcript accumulation of pathogenesis-related proteins at different stages of the interaction. Expression levels are shown relative to the constitutively expressed CYCLOPHILIN2 gene. Error bars indicate SD from three technical replicates. Statistical significance of gene induction in *M. oryzae*–infected versus control roots: *, $P < 0.05$; ***, $P < 0.001$. Gray, white, and black bars correspond to mock-inoculated root samples at 2, 4, and 6 DAI, respectively. Dotted and horizontally and diagonally striped bars refer to *M. oryzae*–infected root samples at 2, 4, and 6 DAI, respectively.

Root Invasion by *M. oryzae* Is Accompanied by Suppression of Defense Response

During the establishment of foliar compatible plant–pathogen interactions, the perception of the pathogen by the plant is accompanied by the induction of a large number of proteins (Tao et al., 2003). By contrast, molecular responses to root infection by pathogens are largely unknown, as are root defense markers. To characterize rice root invasion by *M. oryzae* at the molecular level, we used well-established foliar defense genes. Three members of the pathogenesis-related (Kankanala et al., 2007) gene families PR1 and PR10 were selected that previously had been shown to display strong gene induction during leaf infection by *M. oryzae* (Midoh and Iwata, 1996; Agrawal et al., 2001; McGee et al., 2001). Furthermore, induction mirrored infection dynamics for the two *PR10* genes *RPR10a* (equivalent to *PBZ1*, probenazole-induced) and *RPR10b* (Midoh and Iwata, 1996; McGee et al., 2001). Temporal expression analysis of the three PR genes during root invasion revealed increased transcript accumulation in infected relative to control roots (Figure 4). Transcript levels of the two *PR10* genes were highest at 2 DAI, followed by a reduction in transcript levels at 4 and 6 DAI. Levels of *PR1a* transcript, by contrast, were marginally induced at 6 DAI. Thus, contrary to leaf infection, the gene expression dynamics did not match progressive root invasion. Despite the utility of these genes as leaf defense markers, our data suggest that they are less suitable as markers for root pathogenesis.

This observation and the fact that biotrophic colonization of plant cells by beneficial or pathogenic fungi has been shown to be associated with suppression of plant defense responses (Schulze-Lefert and Panstruga, 2003; Harrison, 2005; Caldo et al., 2006) led us to determine the global transcriptional response of rice roots following the invasion by *M. oryzae*. Infected and noninfected roots were collected at 2, 4, and 6 DAI and transcript accumulation quantified using the Affymetrix rice GeneChip platform. Using a linear model, 2245 features (equivalent to 2009 distinct genes) were identified exhibiting a different expression profile in infected compared with noninfected roots (see Supplemental Data Set 1 online). Principal component analysis (PCA) showed that transcriptome alteration was most pronounced at 2 DAI (Figure 5A, left panel), indicative of a large-scale, early, and transient transcriptional response to infection. Modeling the dynamics of the 2245 features across the two treatments and three time points allowed features to be grouped into six distinct expression profiles (profiles I to VI), of which the largest group, termed profile I, corresponded to 720 features that showed a strong increase in accumulation at 2 DAI with a reduction at the 4 and 6 DAI time points (Figure 5B; see Supplemental Data Set 1 online). Within this category were a large proportion of genes representative of basal defense with some of them already well characterized during leaf infection (Table 1); for example, an endochitinase (Chit1; Kim et al., 2009), an elicitor-inducible shikimate kinase (SK2; Kasai et al., 2005), certain members of the WRKY family (WRKY71, Chujo et al., 2008; WRKY53, Chujo et al., 2009), or noteworthy, the previously described chitin receptor (chitin-elicitor binding protein, CEBiP; Kaku et al., 2006), a Ser/Thr protein kinase previously reported to be associated with defense against biotrophic rust fungi in other cereals (ORK10; Cheng et al., 2002b), and *NAC4*, a transcriptional activator involved in the initiation of hypersensitive response–associated cell death (Kaneda et al., 2009). The distinct gene expression pattern was independently confirmed by real-time RT-PCR (see Supplemental Figure 1 online). The patterns of transcript accumulation of these genes are consistent with perception of the pathogen followed by biotrophy-accompanied defense suppression.

We compared our data to a publicly available Affymetrix data set (GSE7256) generated from *M. oryzae*–infected leaves sampled at 3 and 4 DAI and found that, on average, the expression values of the 720 induced feature candidates, including the previously characterized defense-related genes, remain high in

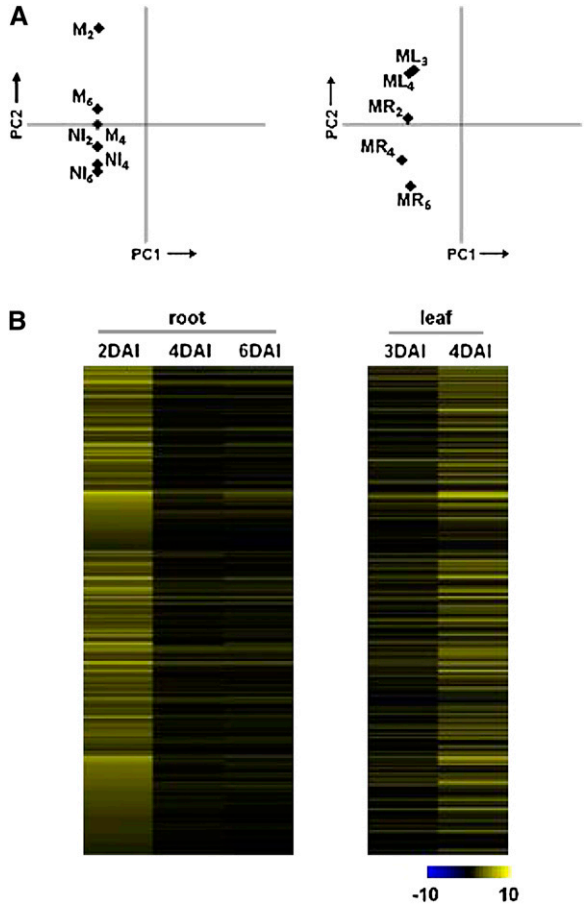

Figure 5. Comparative Analyses of Gene Expression Profiles in Roots and Leaves during *M. oryzae* Infection.

(A) Left, PCA of transcript accumulation levels in *M. oryzae*–infected (M) and noninfected (NI) roots sampled at 2, 4, and 6 DAI (M2, M4, M6 and NI2, NI4, NI6, respectively). Right, PCA of fold change ratios in *M. oryzae*–infected roots (MR) sampled at 2, 4, and 6 DAI, and leaves (ML) sampled at 3 and 4 DAI (MR2, MR4, MR6 and ML3, ML4, respectively) PC1 and PC2, principal components 1 and 2, respectively.

(B) Fold change of transcript accumulation (log_2 units) of 720 transiently induced features in roots and leaves, sampled at 2, 4, and 6 DAI, and 3 and 4 DAI, respectively. Yellow indicates increased level of expression; blue indicates decreased level of expression (scale shown below).

Table 1. Expression of Genes Representative for Plant Defense Response and Cell Death

			Roots			Leaves	
Gene Name	Description	TIGR	2 DAI	4 DAI	6 DAI	3 DAI	4 DAI
CEBiP[a]	Chitin receptor	Os03g04110	2.1	1.2	1.3	3.9	8.0
ORK10[b]	Ser/Thr protein kinase	Os01g02300	8.5	1.5	1.5	0.8	5.6
SK2[c]	Shikimate kinase	Os06g12150	6.7	2.4	1.9	1.1	2.5
WRKY53[d]	Transcription factor	Os05g27730	5.6	1.3	1.5	1.8	3.9
WRKY71[e]	Transcription factor	Os02g08440	17.8	1.5	2.1	9.3	17.1
NAC4[f]	Transcription factor	Os01g60020.1	5.6	2.5	1.7	11.8	36.1
Chit1[g]	Chitinase	Os02g39330	42.6	4.8	5.9	5.1	12.0
JAmyb[h]	Transcription factor	Os11g45740.1	1.6	0.9	1.6	21.4	164.5

Transcript accumulation fold change of infected relative to noninfected tissue at 2, 4, and 6 DAI for roots and 3 and 4 DAI for leaves.
[a]Kaku et al. (2006).
[b]Cheng et al. (2002).
[c]Kasai et al. (2005).
[d]Chujo et al. (2009).
[e]Chujo et al. (2008).
[f]Kaneda et al. (2009).
[g]Kim et al. (2009).
[h]Lee et al. (2001).

leaves at 3 to 4 DAI, and even increase, in the later stages of infection (Figure 5B, Table 1). PCA using all features indicated that the 2 DAI root sample was most similar to the two leaf samples (Figure 5A, right panel). Host transcriptional changes at early stages of root infection are therefore the most similar ones to leaf infection profiles. In addition, features corresponding to a cell death (and thus necrotrophy) marker, the jasmonic acid–inducible myb transcription factor *JAmyb* (Lee et al., 2001; Mosquera et al., 2009), displayed high and increasing expression values in leaves, whereas root invasion did not lead to induction of *JAmyb* (Table 1).

In summary, the transcriptional state of the rice leaf and root tissue upon invasion by *M. oryzae* differs profoundly with basal defense-related transcripts being rapidly, but transiently, induced during the early stages of biotrophic root infection, whereas the same transcripts continue to accumulate at high levels during the hemibiotrophic infection of leaves.

DISCUSSION

We performed a detailed cytological and molecular characterization of rice root invasion by *M. oryzae*. After formation of morphologically distinct penetration structures, namely, melanized appressoria on leaves and simple hyphopodia on roots, colonization of each tissue is comparably efficient regarding fungal spread from the outer epidermal to the inner conductive tissue. On leaves, the fungus penetrates the epidermis at 1 to 1.5 DAI and grows into mesophyll and conductive tissue within 3 to 4 DAI (Berruyer et al., 2006; Wilson and Talbot, 2009). In our study, rhizodermal penetration occurred at 2 to 3 DAI, followed by cortex and stele invasion at 4 and 6 DAI, respectively. Thus, within 3 to 4 d after invasion of the outermost cell layer, the fungus had entered into the conductive tissue of either organ, at which point infection in the leaf is accelerated (Berruyer et al., 2006) and systemic plant infection commences from roots (Sesma and Osbourn, 2004). On its route toward the root vasculature, the fungus progresses intracellularly, displaying limited hyphal branching inside the cells, in contrast to the intense hyphal proliferation that almost entirely fills leaf sheath cells (Kankanala et al., 2007; Mosquera et al., 2009). Root infection by *M. oryzae* was marked by cellular features typical for biotrophic interactions: the presence of a plant-derived membrane surrounding intracellular IH separating fungal from host cytoplasm and a massive constriction of the fungal hyphae when crossing host cells leading to a nondestructive progression of the pathogen within the tissue (Wharton et al., 2001; Harrison et al., 2002; Lagopodi et al., 2002; Panstruga, 2003; Maciá-Vicente et al., 2009). Importantly, in leaf tissue, biotrophic growth is restricted to the front of infection since penetrated cells die once the fungus progresses to the neighboring cells (Kankanala et al., 2007). However, biotrophic invasion of roots is continuous, as demonstrated by living root cells that remain capable of endocytosis along the fungal infection path, indicating the preference for a prolonged asymptomatic growth in roots as opposed to hemibiotrophy on leaves (Berruyer et al., 2006; Kankanala et al., 2007; Wilson and Talbot, 2009). Lesion formation is known to be preceded by the induction of *JAmyb*, a jasmonic acid–inducible Myb transcription factor (Lee et al., 2001; Mosquera et al., 2009). In contrast to many other defense-associated genes, *JAmyb* is also wound induced and therefore linked to cell death per se. The absence of induction of *JAmyb* in *M. oryzae*–infected rice roots therefore provides molecular support for the absence of cell death.

Further support for the occurrence of tissue-specific infection strategies of phytopathological fungi is lent by the recent discovery that *Ustilago maydis*–induced tumor formation on different organs of the maize (*Zea mays*) plant is associated with organ-specific gene expression in maize (and *U. maydis*), including differences in transcript levels of defense genes (Skibbe et al., 2010). Rice root infection by *M. oryzae* must rely on adapted plant transcriptional reprogramming, allowing the

establishment of the biotrophic development of the pathogen (Panstruga, 2003; Schulze-Lefert and Panstruga, 2003; O'Connell and Panstruga, 2006). We observed the early and transient triggering of genes implicated in a nonspecific basal defense response, typical of the perception of pathogen-derived elicitors or pathogen-associated molecular patterns (Boller and Felix, 2009). Constituents of the fungal cell wall, such as chitin and other glucans, have been recognized as conserved pathogen-associated molecular patterns, and we observed transient accumulation of transcripts encoding the chitin receptor CEBiP (for chitin elicitor binding protein) that has previously been shown to play a central role in pathogen recognition (Kaku et al., 2006). The rice Ser/Thr kinase ORK10 was also included, a homolog of the wheat (*Triticum aestivum*) LRK10 (Feuillet et al., 1997) and the oat (*Avena sativa*) ORK10 (Cheng et al., 2002a) proteins that are associated with the response to rust fungi that biotrophically infect plant leaves. During the establishment of a compatible interaction between oat and the rust fungus, transcription of ORK10 becomes suppressed, whereas expression remains high during an incompatible interaction (Cheng et al., 2002a). Similar dynamics of initial induction and subsequent attenuation of defense-related gene expression were observed at early stages of compatible leaf interactions with other biotrophic fungal pathogens, such as between maize and *U. maydis* (Doehlemann et al., 2008) or between barley (*Hordeum vulgare*) and *Blumeria graminis* (causing powdery mildew disease; Caldo et al., 2006). In both interactions, transcriptional reduction coincided with the onset of cell invasion, consistent with the necessity for suppression of basal defense prior differentiation of intracellular fungal feeding structures (O'Connell and Panstruga, 2006). For instance, in the barley–powdery mildew interaction, gene expression profiling revealed an overall repression of defense-related genes during haustoria formation (Caldo et al., 2004, 2006; Gjetting et al., 2007). The dynamics of transcriptional changes in rice roots infected by *M. oryzae* is therefore similar to that of leaves infected by biotrophic fungal pathogens and provides evidence that basal defense in roots can be targeted for suppression by, as yet elusive, fungal pathogen-derived

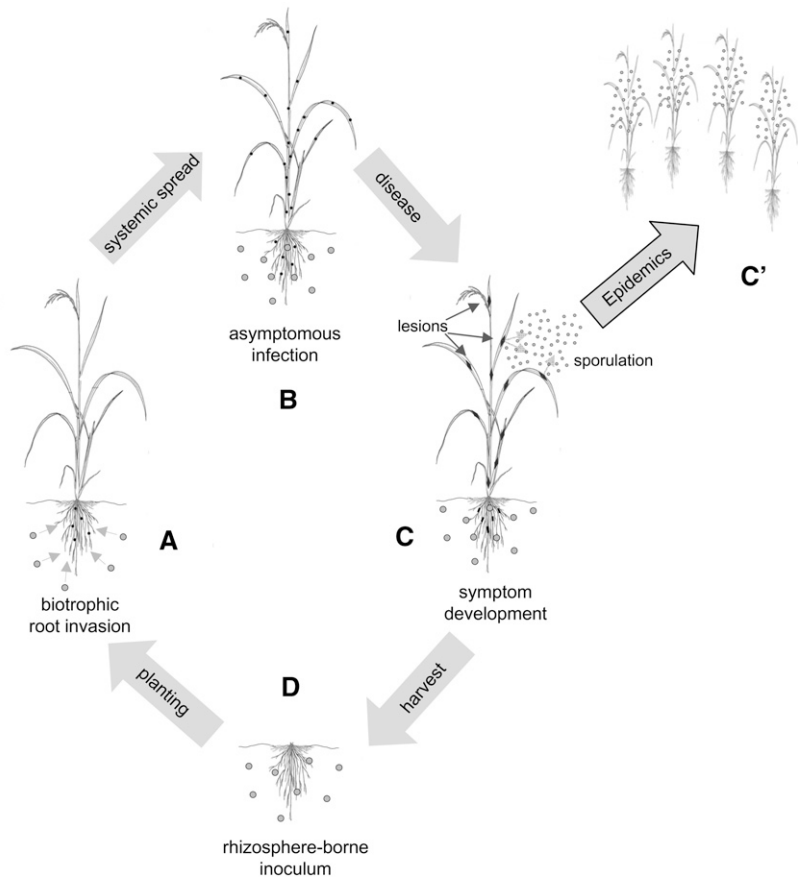

Figure 6. Model of the Epidemiological Life Cycle of *M. oryzae* under Field Conditions.

Root invasion commences from rhizosphere-borne inoculum, such as mycelium-infested plant remnants or microsclerotia **(A)**. Systemic spread of *M. oryzae* that is continuously nourished by a symptomless plant **(B)**. Hyphal infection of the aerial parts of the plant causes disease when the fungus switches to necrotrophic growth, which results in lesion formation **(C)** and produces large amounts of asexual spores, rapidly infecting leaves of other plants leading to the devastating spread of the disease **(C')**. During harvest, infested crop residues and fungal resting structures (microsclerotia) remain in the soil **(D)**, from where biotrophic root invasion of newly planted seedlings can be reinitiated **(A)**.

effector proteins. Although it is still not known whether *M. oryzae* IH share feeding properties with haustoria, comparable plant transcriptional reprogramming may assist intracellular proliferation of IH. Similarly, cellular and molecular evidence has demonstrated modulation of plant defense response during AM symbiosis (Gianinazzi-Pearson et al., 1996; Harrison, 2005), suggesting a common plant response to both symbiotic and pathogenic biotrophs. Commonalities between these two types of interactions have earlier been recognized (Güimil et al., 2005; Paszkowski, 2006); however, the only signaling pathway currently known to be required for intracellular accommodation of root biotrophs, the common SYM signaling pathway, is dispensable for intracellular growth of *M. oryzae.*

The study of leaf biotrophy during *M. oryzae* infection of rice is hampered by the simultaneous presence of necrotrophy. Therefore, it remains technically challenging to focus molecular analyses on the limited number of plant cells that respond specifically to biotrophic invasion. Expression analysis on rice leaf sheath material enriched for intracellular IH recently showed that known defense response–associated genes were moderately induced in this tissue (Mosquera et al., 2009). This transcriptome snapshot does not distinguish between moderate inductions corresponding to temporally static, increasing, or decreasing expression. Transcriptional reprogramming of leaf cells for a transient cell invasion phase might differ from that of the durable biotrophy in roots, which could explain the opposite patterns of expression profiles in roots and leaves observed in this study.

Nevertheless, disease symptoms also develop on roots but occur only after prolonged cocultivation of more than 2 weeks (Dufresne and Osbourn, 2001; Sesma and Osbourn, 2004; Heupel et al., 2010). Similar to *M. oryzae*, the hemibiotrophic pathogen *Colletotrichum graminicola*, which causes anthracnose leaf blight in maize, also infects roots and spreads to aerial parts of the plant; however, the fungal lifestyle in roots is unknown (Sukno et al., 2008). In addition, *C. graminicola* rapidly switches to necrotrophic growth within the first 3 DAI during foliar infection but requires 42 DAI to develop symptoms on roots. It is not known which plant and/or fungal signals trigger the differentiation of IH into necrotrophic hyphae (Wilson and Talbot, 2009), but these might differ between leaf and root infection events. The formation of disease lesions on aboveground plant parts presents a spore-dispersal platform exposed to wind or dewdrop splash for rapid aboveground spread, whereas belowground spreading is necessarily less efficient. It is tempting to speculate that fungal entrance via the root tissue followed by spreading in an asymptomatic fashion, as observed for *M. oryzae*, permits continuous nourishment of the fungus by healthy host tissue until the fungus reaches the aerial parts of the plant for profuse sporulation (Figure 6; Talbot and Kershaw, 2009). New seedling infestations after winter or crop rotation periods are unlikely to occur from conidia as a source of inoculum (Valent, 2004). Instead fungal inoculum conserved in the soil in the form of mycelium on plant remnants (e.g., straw or seed; Ou, 1985; Long et al., 2001) or, alternatively, resting structures (microsclerotia) might set the infection cycle in motion starting from roots as a primary port of entry (Figure 6; Sesma and Osbourn, 2004; Valent, 2004). The omnipresence of rice blast wherever rice is cultivated (http://www.knowledgebank.irri.org) lends further support to this model. Also, brusone, the presently rapidly spreading wheat blast disease of South America, is caused by *M. oryzae* and results in bleached (sterile) ears of wheat plants. Interestingly, upon plant exposure to the respective temperature and wetting regimes, symptom development can be either suppressed to 0% or enhanced to 85% of the treated plants (Cardoso et al., 2008), consistent with the asymptomatic infection of the plant body by *M. oryzae* prior to environmental stimulation of disease outbreak. The tissue for primary infection of wheat blast is not known, but disease dissemination transmitted by contaminated seeds that are present in the soil and serve as a potent inoculum has been reported and thus represents a plausible explanation for field contamination (Urashima et al., 1999, 2009).

It will be an exciting future challenge to determine the molecular mechanisms underpinning the biotrophy and the switch to necrotrophy of *M. oryzae* in leaves and roots and to elucidate the support of roots for asymptomatic proliferation of *M. oryzae* relative to leaves. Most importantly, the epidemiological significance of blast root infection needs to be addressed forthwith. Possibly, newly developed disease control strategies aimed at efficiently combating the blast disease in rice as well as in wheat need to include considering roots as a port of entry for the pathogenic fungus.

METHODS

Plant and Fungal Material

Wild-type japonica rice (*Oryza sativa* cv Nipponbare and cv Dongjin) and mutant lines (Jeong et al., 2002, 2006; Miyao et al., 2003) 1B-08643 and NF8513 mutated in *CASTOR* and *CCaMK* (Gutjahr et al., 2008), respectively, were used in this study. GFP-expressing *Magnaporthe oryzae* strain Guy11 (Talbot et al., 1993), courtesy of Ane Sesma (John Innes Centre, UK), was used for all experiments.

Inoculation Conditions

Rice seeds were surface sterilized as described (Gutjahr et al., 2008), aligned on sterile water/0.6% plant agar, and incubated vertically at 30°C in the dark for 4 d to promote root growth. Plants were then grown vertically in a controlled environment growth chamber with a 16-h-light/8-h-dark photoperiod at 28/24°C for another 6 d. Infection assays were conducted on roots laid on sterile filter paper placed on fresh water/0.6% plant agar. *M. oryzae* mycelium was cultured at 26°C on solid Complete Medium (Talbot et al., 1993) with a 16-h-light/8-h-dark photoperiod, and conidia were harvested from 8-d-old cultures by rinsing mycelium several times with a sterile solution of 0.1% Tween20 and 0.01% antifoam A (Sigma-Aldrich). Each plate of four to six plants received a total of 5.10^4 conidia randomly distributed on top of the root system. Sterile 0.1% Tween 20 and 0.01% antifoam A solution was used for mock inoculation. Inoculated plants were kept horizontally at 26°C with a 16-h-light/8-h-dark photoperiod. Homozygote mutants *castor-1* and *ccamk-2* were selected from segregating seedlings by PCR as described (Gutjahr et al., 2008).

Microscopy Inspection of Root Infection

Root infection by *M. oryzae* was monitored over time using a Leica MZ16FA stereomicroscope equipped with a UV lamp. The progression of *M. oryzae* was followed at 15 marked inoculation sites per plate and a total of two plates at 2, 4, and 6 DAI. For detailed inspection, root tissue was observed on a Leica TCS SP2 AOBS confocal microscope. Root

samples were treated for 5 min with 15 μM propidium iodide (Sigma-Aldrich) to reveal plant cell walls. Independently, membranes were stained with 16 μM FM4-64 dye (Invitrogen) for 20 min. Fluorescence of GFP, propidium iodide, and FM4-64 was detected using an excitation wavelength of 488 nm. Signals emitted from GFP, propidium iodide, and FM4-64 were recorded in two specific emission windows of 510 to 550 nm for GFP and 600 to 650 nm for propidium iodide and FM4-64. *M. oryzae*- and mock-inoculated roots harvested at 6 DAI were stained with trypan blue as described (Brundrett et al., 1984). For electron microscopy, 2-mm-long root segments harvested at 8 DAI were fixed overnight at room temperature in 2% (w/v) paraformaldehyde and 2.5% (v/v) glutaraldehyde in phosphate buffer (0.1 M, pH 7.4). Specimens were washed in phosphate buffer (0.1 M, pH 7.4) and postfixed in 1% (w/v) osmium tetroxide for 1.5 h at room temperature. After several washes in distilled water, specimens were dehydrated progressively through an ethanol series. Specimens were then washed with propylene oxide and embedded in Epon-Araldite resin in flat embedding molds. Ultrathin sections were counterstained with lead citrate and observed with a Philips CM-10 transmission electron microscope.

RNA Extraction, cDNA Synthesis, and Real-Time RT-PCR

RNA was extracted from roots infected (M) or not infected (NI) with *M. oryzae* at 2, 4, and 6 d after infection and amplified using the Nugen-ovation Pico kit (Nugen) as per the manufacturer's instructions. cDNA synthesis and real-time RT-PCR were performed as described earlier (Gutjahr et al., 2008). Primer sequence design for real-time RT-PCR was adopted from (Güimil et al., 2005). Primer sequences to quantify *M. oryzae* were retrieved from (Qi and Yang, 2002), and all primer sequences are listed in Supplemental Table 1 online. The absence of contaminating genomic DNA was confirmed by performing a control PCR on RNA not reverse transcribed (-RT). Expression values were calculated according to Güimil et al. (2005) and normalized as previously described (Gutjahr et al., 2008) to the geometric mean of amplification of three nearly constitutively expressed genes: CYCLOPHILIN2, GAPDH, and POLYUBIQUITIN. Normalized expression values were displayed as a function of CYCLOPHILIN2 expression. A gene was defined as induced after applying the Student's *t* test with a false discovery rate <0.05.

Microarray Analysis

Two independent biological replicates were performed, giving a total of 12 samples, and biotin-labeled cDNA was hybridized to Affymetrix rice Genechips as previously described (Güimil et al., 2005). For analysis, data were normalized using the RMA function in the *affy* Bioconductor package (http://bioconductor.fhcrc.org/) for R statistics software (http://www.r-project.org/). PCA was conducted using whole-genome expression data for the comparison of root samples or fold change values for the comparison between leaf and root samples.

Gene expression variation was analyzed using a fixed-effects linear model. For any given feature (*f*), the normalized expression value Y_{ftir} was modeled as,

$$Y_{ftir} = \beta_0 + \beta_1 Day_t + \beta_2 Infection_i + \beta_3 Day_t \times Infection_i + \varepsilon_{ftir} \quad (1)$$

where Day_t is the time after infection for t = 2, 4, or 6 d, $Infection_i$ is the infection status for i = 0, noninfected and i = 1, infected roots, f is the feature number from 1 to F, r is the replicated number 1 or 2, ε_{ftir} is the error term, and $\beta_{0\text{-}3}$ are parameters to be estimated. Infection-regulated genes were identified on the basis of noncoincidence of the regression lines corresponding to noninfected and infected samples (rejection of H_0: $\beta_2 = \beta_3 = 0$) (i.e., a difference in either intercept or slope). Q-values were obtained for the resulting set of P values using the Bioconductor Q-value package for R and regulated genes identified at 5% false discovery rate control. An additional fold change cutoff of ± 1 $\log_2$ fold change was applied on the basis of the maximum fold change observed across the three time points, resulting in a candidate gene list of 2245 features (see Supplemental Data Set 1 online). Selected features were further classified as upregulated (1404 features) or downregulated (841 features) following the sign of the maximum fold change. Features were additionally classified as dynamically regulated based on the difference in slope between noninfected and infected samples (rejection of H_0:$\beta_3 = 0$). To increase the ability to detect significance of the interaction term (β_3), Q-values were calculated using only the previously selected features, resulting in the identification of 1642 dynamically regulated features. The sign of the difference in slope ($\beta_3 - \beta_1$) was used to classify further features as increasing or decreasing in differential regulation over time. A total of 720 features that were classified as upregulated with a negative slope difference (infected–noninfected) were defined as transiently induced following infection.

For comparative analysis of root and leaf infection, expression of the 720 features was examined in a publically available Affymetrix data set obtained from *Magnaporthe*-infected leaves, harvested 3 and 4 DAI. Features changing by ± 1 $\log_2$ fold change between 3 and 4 DAI were classified as increasing, or decreasing, respectively. On this basis, 301 features were called as increasing in leaves and 26 as decreasing. Global PCA of leaf and root treatments was conducted as described above using fold change measures. Only the first two components are shown in Figure 5.

Accession Numbers

Sequence data from this article can be found in The Institute for Genomic Research or GenBank/EMBL databases under the following accession numbers: CYCLOPHILIN2, LOC_Os02g02890; GAPDH, LOC_Os08g03290; POLYUBIQUITIN, LOC_Os06g46770; CEBiP, LOC_Os03g04110; ORK10, Os01g02300; SK2, Os06g12150; WRKY53, Os05g27730; WRKY71, Os02g08440; and Chit1, Os02g39330. The complete data set is accessible through the Gene Expression Omnibus Series accession numbers GSE18361 and GSE7256.

Supplemental Data

The following materials can be found in the online version of this article.

Supplemental Figure 1. Real-Time RT-PCR–Based Temporal Expression Analysis of Class I Genes Representative of Rice Defense Response.

Supplemental Table 1. Primer Sequences for Real-Time RT-PCR.

Supplemental Data Set 1. List of Genes Exhibiting a Different Expression Profile in Infected Compared with Noninfected Roots.

ACKNOWLEDGMENTS

We thank Caroline Gutjahr for critical reading of the manuscript and for many stimulating discussions. Ane Sesma provided us with many helpful suggestions during the establishment of the rice root infection protocol. We thank Jean Daraspe, Niko Geldner, and Hannes Richter for assistance with transmission electron microscopy, confocal laser scanning microscopy, and real-time RT-PCR, respectively. We appreciate the helpful suggestions of an anonymous reviewer and the coeditor. The work was funded by the Swiss National Science Foundation "professeur boursier" Grant PP00A-110874. S.M. was supported by the Swiss Ministry of Environmental Affairs (StoBoBio/2004.H 12i).

Received July 9, 2010; revised September 2, 2010; accepted September 7, 2010; published September 21, 2010.

REFERENCES

Agrawal, G., Rakwal, R., Jwa, N., and Agrawal, V. (2001). Signaling molecules and blast pathogen attck activates rice OsPR1a and OsPR1b genes: A model illustrating components participating during defense/stress response. Plant Physiol. Biochem. **39:** 1095–1103.

Asher, M., and Shipton, P. (1981). Biology and Control of Take-All. (London: Academic Press).

Berrocal-Lobo, M., and Molina, A. (2004). Ethylene response factor 1 mediates Arabidopsis resistance to the soilborne fungus *Fusarium oxysporum*. Mol. Plant Microbe Interact. **17:** 763–770.

Berruyer, R., Poussier, S., Kankanala, P., Mosquera, G., and Valent, B. (2006). Quantitative and qualitative influence of inoculation methods on in planta growth of rice blast fungus. Phytopathology **96:** 346–355.

Boller, T., and Felix, G. (2009). A renaissance of elicitors: Perception of microbe-associated molecular patterns and danger signals by pattern-recognition receptors. Annu. Rev. Plant Biol. **60:** 379–406.

Bolte, S., Talbot, C., Boutte, Y., Catrice, O., Read, N.D., and Satiat-Jeunemaitre, B. (2004). FM-dyes as experimental probes for dissecting vesicle trafficking in living plant cells. J. Microsc. **214:** 159–173.

Brundrett, M.C., Piché, Y., and Peterson, R.L. (1984). A new method for observing the morphology of vesicular-arbuscular mycorrhizae. Can. J. Bot. **62:** 2128–2134.

Caldo, R.A., Nettleton, D., Peng, J., and Wise, R.P. (2006). Stage-specific suppression of basal defense discriminates barley plants containing fast- and delayed-acting Mla powdery mildew resistance alleles. Mol. Plant Microbe Interact. **19:** 939–947.

Caldo, R.A., Nettleton, D., and Wise, R.P. (2004). Interaction-dependent gene expression in Mla-specified response to barley powdery mildew. Plant Cell **16:** 2514–2528.

Cannon, P. (1994). The newly recognized family Magnaporthaceae and its interrelationships. Systema Ascomycetum **13:** 25–42.

Cardoso, C.A.A., Reis, E.M., and Moreira, E.N. (2008). Development of a warning system for wheat blast caused by *Pyricularia grisea*. Summa Phytopathol. **34:** 216–221.

Cheng, D.W., Armstrong, K.C., Tinker, N., Wight, C.P., He, S., Lybaert, A., Fedak, G., and Molnar, S.J. (2002b). Genetic and physical mapping of Lrk10-like receptor kinase sequences in hexaploid oat (*Avena sativa* L.). Genome **45:** 100–109.

Cheng, D.W., He, S., and Armstrong, K.C. (2002a). Modified expression of two receptor kinase genes in hexaploid oat (*Avena sativa* L.) on inoculation with crown rust. Physiol. Mol. Plant Pathol. **61:** 281–288.

Chujo, T., et al. (2008). Characterization of an elicitor-induced rice WRKY gene, OsWRKY71. Biosci. Biotechnol. Biochem. **72:** 240–245.

Chujo, T., Sugioka, N., Masuda, Y., Shibuya, N., Takemura, T., Okada, K., Nojiri, H., and Yamane, H. (2009). Promoter analysis of the elicitor-induced WRKY gene OsWRKY53, which is involved in defense responses in rice. Biosci. Biotechnol. Biochem. **73:** 1901–1904.

Doehlemann, G., Wahl, R., Horst, R.J., Voll, L.M., Usadel, B., Poree, F., Stitt, M., Pons-Kühnemann, J., Sonnewald, U., Kahmann, R., and Kämper, J. (2008). Reprogramming a maize plant: Transcriptional and metabolic changes induced by the fungal biotroph *Ustilago maydis.* Plant J. **56:** 181–195.

Dufresne, M., and Osbourn, A.E. (2001). Definition of tissue-specific and general requirements for plant infection in a phytopathogenic fungus. Mol. Plant Microbe Interact. **14:** 300–307.

Farman, M.L., Eto, Y., Nakao, T., Tosa, Y., Nakayashiki, H., Mayama, S., and Leong, S.A. (2002). Analysis of the structure of the AVR1-CO39 avirulence locus in virulent rice-infecting isolates of *Magnaporthe grisea.* Mol. Plant Microbe Interact. **15:** 6–16.

Feuillet, C., Schachermayr, G., and Keller, B. (1997). Molecular cloning of a new receptor-like kinase gene encoded at the *Lr10* disease resistance locus of wheat. Plant J. **11:** 45–52.

Gianinazzi-Pearson, V., Dumas-Gaudot, E., Gollotte, A., Tahiri-Alaoui, A., and Gianinazzi, S. (1996). Cellular and molecular defence-related root responses to invasion by arbuscular mycorrhizal fungi. New Phytol. **133:** 45–57.

Gjetting, T., Hagedorn, P.H., Schweizer, P., Thordal-Christensen, H., Carver, T.L.W., and Lyngkjaer, M.F. (2007). Single-cell transcript profiling of barley attacked by the powdery mildew fungus. Mol. Plant Microbe Interact. **20:** 235–246.

Glazebrook, J. (2005). Contrasting mechanisms of defense against biotrophic and necrotrophic pathogens. Annu. Rev. Phytopathol. **43:** 205–227.

Güimil, S., Chang, H.-S., Zhu, T., Sesma, A., Osbourn, A., Roux, C., Ioannidis, V., Oakeley, E.J., Docquier, M., Descombes, P., Briggs, S.P., and Paszkowski, U. (2005). Comparative transcriptomics of rice reveals an ancient pattern of response to microbial colonization. Proc. Natl. Acad. Sci. USA **102:** 8066–8070.

Gutjahr, C., Banba, M., Croset, V., An, K., Miyao, A., An, G., Hirochika, H., Imaizumi-Anraku, H., and Paszkowski, U. (2008). Arbuscular mycorrhiza-specific signaling in rice transcends the common symbiosis signaling pathway. Plant Cell **20:** 2989–3005.

Gutjahr, C., Casieri, L., and Paszkowski, U. (2009). *Glomus intraradices* induces changes in root system architecture of rice independently of common symbiosis signaling. New Phytol. **182:** 829–837.

Harrison, M.J. (2005). Signaling in the arbuscular mycorrhizal symbiosis. Annu. Rev. Microbiol. **59:** 19–42.

Harrison, M.J., Dewbre, G.R., and Liu, J. (2002). A phosphate transporter from *Medicago truncatula* involved in the acquisition of phosphate released by arbuscular mycorrhizal fungi. Plant Cell **14:** 2413–2429.

Hermanns, M., Slusarenko, A.J., and Schlaich, N.L. (2003). Organ-specificity in a plant disease is determined independently of R gene signaling. Mol. Plant Microbe Interact. **16:** 752–759.

Heupel, S., Roser, B., Kuhn, H., Lebrun, M.H., Villalba, F., and Requena, N. (2010). Erl1, a novel era-like GTPase from *Magnaporthe oryzae*, is required for full root virulence and is conserved in the mutualistic symbiont *Glomus intraradices*. Mol. Plant Microbe Interact. **23:** 67–81.

Jeong, D.-H., An, S., Kang, H.-G., Moon, S., Han, J.-J., Park, S., Lee, H.S., An, K., and An, G. (2002). T-DNA insertional mutagenesis for activation tagging in rice. Plant Physiol. **130:** 1636–1644.

Jeong, D.-H., et al. (2006). Generation of a flanking sequence-tag database for activation-tagging lines in japonica rice. Plant J. **45:** 123–132.

Kaku, H., Nishizawa, Y., Ishii-Minami, N., Akimoto-Tomiyama, C., Dohmae, N., Takio, K., Minami, E., and Shibuya, N. (2006). Plant cells recognize chitin fragments for defense signaling through a plasma membrane receptor. Proc. Natl. Acad. Sci. USA **103:** 11086–11091.

Kaneda, T., Taga, Y., Takai, R., Iwano, M., Matsui, H., Takayama, S., Isogai, A., and Che, F.-S. (2009). The transcription factor OsNAC4 is a key positive regulator of plant hypersensitive cell death. EMBO J. **28:** 926–936.

Kankanala, P., Czymmek, K., and Valent, B. (2007). Roles for rice membrane dynamics and plasmodesmata during biotrophic invasion by the blast fungus. Plant Cell **19:** 706–724.

Kasai, K., Kanno, T., Akita, M., Ikejiri-Kanno, Y., Wakasa, K., and Tozawa, Y. (2005). Identification of three shikimate kinase genes in rice: Characterization of their differential expression during panicle development and of the enzymatic activities of the encoded proteins. Planta **222:** 438–447.

Kim, S.T., Kang, Y.H., Wang, Y., Wu, J., Park, Z.Y., Rakwal, R., Agrawal, G.K., Lee, S.Y., and Kang, K.Y. (2009). Secretome analysis of differentially induced proteins in rice suspension-cultured

cells triggered by rice blast fungus and elicitor. Proteomics **9:** 1302–1313.

Kimbrough, J.M., Salinas-Mondragon, R., Boss, W.F., Brown, C.S., and Sederoff, H.W. (2004). The fast and transient transcriptional network of gravity and mechanical stimulation in the Arabidopsis root apex. Plant Physiol. **136:** 2790–2805.

Lagopodi, A.L., Ram, A.F.J., Lamers, G.E.M., Punt, P.J., Van den Hondel, C.A.M.J.J., Lugtenberg, B.J.J., and Bloemberg, G.V. (2002). Novel aspects of tomato root colonization and infection by *Fusarium oxysporum* f. sp. *radicis-lycopersici* revealed by confocal laser scanning microscopic analysis using the green fluorescent protein as a marker. Mol. Plant Microbe Interact. **15:** 172–179.

Landschoot, P., and Jackson, N. (1989). *Magnaporthe poae* sp. nov., a hyphopodiate fungus with a *Phialophora* anamorph from grass roots in the United States. Mycol. Res. **93:** 59–62.

Lee, M.-W., Qi, M., and Yang, Y. (2001). A novel jasmonic acid-inducible rice myb gene associates with fungal infection and host cell death. Mol. Plant Microbe Interact. **14:** 527–535.

Lewis, D.H. (1973). Concepts in fungal nutrition and the origin of biotrophy. Biol. Rev. Camb. Philos. Soc. **48:** 261–277.

Long, D., Correll, J., Lee, F., and TeBeest, D. (2001). Rice blast epidemics initiated by infested rice grain on the soil surface. Plant Dis. **85:** 612–616.

Maciá-Vicente, J.G., Jansson, H.B., Talbot, N.J., and Lopez-Llorca, L.V. (2009). Real-time PCR quantification and live-cell imaging of endophytic colonization of barley (*Hordeum vulgare*) roots by *Fusarium equiseti* and *Pochonia chlamydosporia.* New Phytol. **182:** 213–228.

McGee, J., Hamer, J., and Hodges, T. (2001). Characterization of a PR-10 pathogenesis-related gene family induced in rice during infection with *Magnaporthe grisea*. Mol. Plant Microbe Interact. **14:** 877–886.

Midoh, N., and Iwata, M. (1996). Cloning and characterization of a probenazole-inducible gene for an intracellular pathogenesis related protein in rice. Plant Cell Physiol. **37:** 9–18.

Miyao, A., Tanaka, K., Murata, K., Sawaki, H., Takeda, S., Abe, K., Shinozuka, Y., Onosato, K., and Hirochika, H. (2003). Target site specificity of the Tos17 retrotransposon shows a preference for insertion within genes and against insertion in retrotransposon-rich regions of the genome. Plant Cell **15:** 1771–1780.

Mosquera, G., Giraldo, M.C., Khang, C.H., Coughlan, S., and Valent, B. (2009). Interaction transcriptome analysis identifies *Magnaporthe oryzae* BAS1-4 as biotrophy-associated secreted proteins in rice blast disease. Plant Cell **21:** 1273–1290.

Munch, S., Lingner, U., Floss, D.S., Liudwig, N., Sauer, N., and Deising, H.B. (2008). The hemibiotrophic lifestyle of *Colletotrichum* species. J. Plant Physiol. **165:** 41–51.

O'Connell, R.J., and Panstruga, R. (2006). Tete a tete inside a plant cell: Establishing compatibility between plants and biotrophic fungi and oomycetes. New Phytol. **171:** 699–718.

Ou, S. (1985). Rice Diseases. (Kew, Surrey, UK: Commonwealth Mycological Institute).

Panstruga, R. (2003). Establishing compatibility between plants and obligate biotrophic pathogens. Curr. Opin. Plant Biol. **6:** 320–326.

Parniske, M. (2000). Intracellular accommodation of microbes by plants: A common developmental program for symbiosis and disease? Curr. Opin. Plant Biol. **3:** 320–328.

Parniske, M. (2008). Arbuscular mycorrhiza: The mother of plant root endosymbioses. Nat. Rev. Microbiol. **6:** 763–775.

Paszkowski, U. (2006). Mutualism and parasitism: The yin and yang of plant symbioses. Curr. Opin. Plant Biol. **9:** 364–370.

Perfect, S.E., and Green, J.R. (2001). Infection structures of biotrophic and hemibiotrophic fungal plant pathogens. Mol. Plant Pathol. **2:** 101–108.

Qi, M., and Yang, Y. (2002). Quantification of *Magnaporthe grisea* during infection of rice plants using real-time polymerase chain reaction and Northern blot/phosphoimaging analyses. Phytopathology **92:** 870–876.

Rebouillat, J., Dievart, A., Verdeil, J., Escoute, J., Giese, G., Breitler, J., Gantet, P., Espeout, S., Guiderdoni, E., and Périn, C. (2009). Molecular genetics of rice root development. Rice **2:** 15–34.

Schulze-Lefert, P., and Panstruga, R. (2003). Establishment of biotrophy by parasitic fungi and reprogramming of host cells for disease resistance. Annu. Rev. Phytopathol. **41:** 641–667.

Sesma, A., and Osbourn, A.E. (2004). The rice leaf blast pathogen undergoes developmental processes typical of root-infecting fungi. Nature **431:** 582–586.

Skibbe, D.S., Doehlemann, G., Fernandes, J., and Walbot, V. (2010). Maize tumors caused by *Ustilago maydis* require organ-specific genes in host and pathogen. Science **328:** 89–92.

Sukno, S.A., Garcia, V.M., Shaw, B.D., and Thon, M.R. (2008). Root infection and systemic colonization of maize by *Colletotrichum graminicola.* Appl. Environ. Microbiol. **74:** 823–832.

Talbot, N.J. (2003). On the trail of a cereal killer: Exploring the biology of *Magnaporthe grisea*. Annu. Rev. Microbiol. **57:** 177–202.

Talbot, N.J., and Kershaw, M.J. (2009). The emerging role of autophagy in plant pathogen attack and host defence. Curr. Opin. Plant Biol. **12:** 444–450.

Talbot, N.J., Ebbole, D.J., and Hamer, J.E. (1993). Identification and characterization of MPG1, a gene involved in pathogenicity from the rice blast fungus *Magnaporthe grisea*. Plant Cell **5:** 1575–1590.

Tao, Y., Xie, Z., Chen, W., Glazebrook, J., Chang, H.S., Han, B., Zhu, T., Zou, G., and Katagiri, F. (2003). Quantitative nature of *Arabidopsis* responses during compatible and incompatible interactions with the bacterial pathogen *Pseudomonas syringae*. Plant Cell **15:** 317–330.

Tucker, S.L., Besi, M.I., Galhano, R., Franceschetti, M., Goetz, S., Lenhert, S., Osbourn, A., and Sesma, A. (2010). Common genetic pathways regulate organ-specific infection-related development in the rice blast fungus. Plant Cell **22:** 953–972.

Urashima, A.S., Grosso, C.R.F., Stabili, A., Freitas, E.G., Silva, C.P., Netto, D.C.S., Franco, I., and Bottan, J.H.M. (2009). Effect of *Magnaporthe grisea* on seed germination, yield and quality of wheat. In Advances in Genetics, Genomics and Control of Rice Blast Disease, G.L. Wang and B. Valent, eds (Dordrecht, The Netherlands: Springer), pp. 267–277.

Urashima, A.S., Hashimoto, Y., Don, L.D., Kusaba, M., Tosa, Y., Nakayashiki, H., and Mayama, S. (1999). Molecular analysis of the wheat blast population in Brazil with a homolog of retrotransposon MGR583. Ann Phytopathol Soc Jpn. **65:** 429–436.

Valent, B. (2004). Plant disease: Underground life for rice foe. Nature **431:** 516–517.

Valent, B., Farrall, L., and Chumley, F.G. (1991). *Magnaporthe grisea* genes for pathogenicity and virulence identified through a series of backcrosses. Genetics **127:** 87–101.

Wharton, P.S., Julian, A.M., and O'Connell, R.J. (2001). Ultrastructure of the infection of *Sorghum bicolor* by *Colletotrichum sublineolum.* Phytopathology **91:** 149–158.

Wilson, R.A., and Talbot, N.J. (2009). Under pressure: Investigating the biology of plant infection by *Magnaporthe oryzae.* Nat. Rev. Microbiol. **7:** 185–195.